energies

Article

Assessing the Potential of a Hybrid Renewable Energy System: MSW Gasification and a PV Park in Lobito, Angola

Salomão Joaquim [1], Nuno Amaro [1,2,3] and Nuno Lapa [4,*]

[1] Department of Electrical and Computer Engineering, NOVA School of Science and Technology, NOVA University Lisbon, 2829-516 Caparica, Portugal; s.joaquim@alumni.fct.unl.pt (S.J.); nuno.amaro@fct.unl.pt (N.A.)
[2] UNINOVA, NOVA School of Science and Technology, NOVA University Lisbon, 2829-516 Caparica, Portugal
[3] LASI, NOVA School of Science and Technology, NOVA University Lisbon, 2829-516 Caparica, Portugal
[4] LAQV-REQUIMTE, Department of Chemistry, NOVA School of Science and Technology, NOVA University Lisbon, Departmental Building, 2829-516 Caparica, Portugal
* Correspondence: ncsn@fct.unl.pt

Abstract: This study investigates a hybrid renewable energy system combining the municipal solid waste (MSW) gasification and solar photovoltaic (PV) for electricity generation in Lobito, Angola. A fixed-bed downdraft gasifier was selected for MSW gasification, where the thermal decomposition of waste under controlled air flow produces syngas rich in CO and H_2. The syngas is treated to remove contaminants before powering a combined cycle. The PV system was designed for optimal energy generation, considering local solar radiation and shading effects. Simulation tools, including Aspen Plus v11.0, PVsyst v8, and HOMER Pro software 3.16.2, were used for modeling and optimization. The hybrid system generates 62 GWh/year of electricity, with the gasifier contributing 42 GWh/year, and the PV system contributing 20 GWh/year. This total energy output, sufficient to power 1186 households, demonstrates an integration mechanism that mitigates the intermittency of solar energy through continuous MSW gasification. However, the system lacks surplus electricity for green hydrogen production, given the region's energy deficit. Economically, the system achieves a Levelized Cost of Energy of 0.1792 USD/kWh and a payback period of 16 years. This extended payback period is mainly due to the hydrogen production system, which has a low production rate and is not economically viable. When excluding H_2 production, the payback period is reduced to 11 years, making the hybrid system more attractive. Environmental benefits include a reduction in CO_2 emissions of 42,000 t/year from MSW gasification and 395 t/year from PV production, while also addressing waste management challenges. This study highlights the mechanisms behind hybrid system operation, emphasizing its role in reducing energy poverty, improving public health, and promoting sustainable development in Angola.

Keywords: green H_2; hybrid system; municipal solid waste gasification; photovoltaic system

Academic Editors: Roberta Roberto and Viviana Negro

Received: 10 May 2025
Revised: 7 June 2025
Accepted: 10 June 2025
Published: 13 June 2025

Citation: Joaquim, S.; Amaro, N.; Lapa, N. Assessing the Potential of a Hybrid Renewable Energy System: MSW Gasification and a PV Park in Lobito, Angola. *Energies* **2025**, *18*, 3125. https://doi.org/10.3390/en18123125

1. Introduction

The growing global demand for energy, driven by population growth and industrialization, continues to rely heavily on non-renewable sources, accounting for over 80% of primary energy consumption (Table 1) [1].

Table 1. Total primary consumption of renewable and non-renewable energies worldwide in 2023 [1].

Energy Source	Consumption in 2023 (%)
Crude	31.70
Coal	26.47
Natural gas	23.30
Hydropower	6.40
Other renewable energies	8.16
Nuclear (non-renewable source)	4.00

As can be seen in Figure 1, in Angola, despite the predominance of hydropower in the energy mix (74.62%), electrification rates remain critically low, with only 42.8% coverage in urban areas and less than 10% in rural regions. This has led to widespread reliance on costly and polluting diesel generators [2,3].

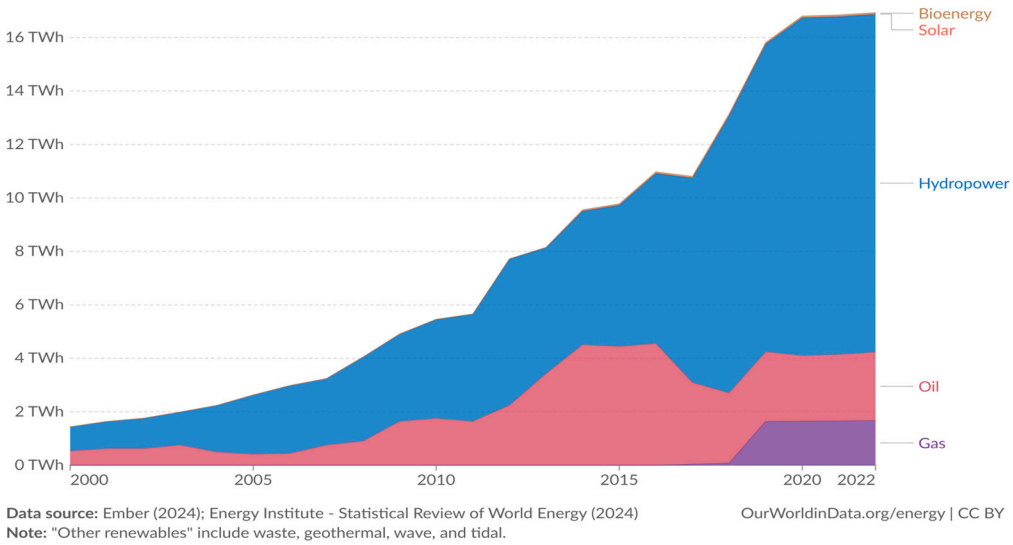

Figure 1. Electricity production by sources in Angola [2].

Poorly managed municipal solid waste (MSW) exacerbates public health risks, contributing to endemic diseases caused by exposure to harmful compounds. Addressing these challenges requires innovative solutions that simultaneously mitigate environmental, energy, and public health issues. Hybrid renewable energy systems, integrating MSW gasification with solar photovoltaic (PV) technology, offer a promising pathway. The synergies between these sources ensure reliability, reduce intermittency, and promote energy security [4–7].

Freris and Infield [8] point out that the synergies between different renewable sources are clearly too important to ignore and can often make the combined exploitable potential greater than the sum of the parts considered in isolation. Soudagar et al. [9] indicate that hybrid systems complement each other to overcome the variable nature of renewable energy sources, such as solar and wind energy, and that, in conjunction with the storage system, they can improve system reliability, energy security, and sustainability. Lee et al. [10] and Alhijazi et al. [11] corroborate this, describing that single-source energy systems (PV and wind) can be unreliable and inefficient in terms of costs, given their intermittent availability, which interrupts the permanent supply of energy. Hybrid systems, on the other hand, increase energy storage capacity, reduce the cost of energy production, improve power quality, and increase total energy efficiency.

The use of MSW, for example, to generate energy helps to avoid the intermittency of a single-source renewable energy system if both sources are combined [10]. These hybrid

systems also offer greater flexibility in the use of local renewable resources and have a higher potential for local employment.

El-Sattar et al. [12] carried out a study on an optimal hybrid system design of PV units, biomass gasification, an electrolyzer, and a fuel cell, for a remote area in Egypt, to meet the electricity demand, with a peak load of 420 kW. The study was developed using algorithms conducted in MATLAB and applied to solve the optimization problem related to the suggested configuration.

Another study was carried out in Egypt by El-Sattar et al. [13], which aimed to size a hybrid off-grid PV system with biomass gasification and a battery, using a quantum model of the Runge–Kutta optimization algorithm. The results showed that the modification algorithm gives the best fitness function in terms of costs of energy, net present cost, and loss of power supply probability.

Cano et al. [14] conducted a techno-economic assessment of a hybrid energy system in an isolated area of Ecuador using HOMER Pro v3.16.2 software. The system integrated 5 kW hydrokinetic turbines, 140 PV panels (35 kWp), batteries, and 70 kWe biomass gasifiers, which powered a 110 kWh gas microturbine to ensure electricity availability when solar and hydrokinetic sources were insufficient. The results confirmed the system's feasibility by demonstrating reliable energy production, cost-effectiveness, and enhanced stability through diversified energy sources.

The study by Campos et al. [15] evaluated a biomass–solar hybrid renewable energy system for João Pinheiro City (Brazil), using Ebsilon Professional software. It focused on energy, economic, and ecological aspects. The system achieved an overall energy efficiency of 17.43% and a Levelized Cost of Energy (LCOE) of 0.034 USD/kWh. The eco-efficiency indicator showed the environmental benefits of this system.

Another study carried out with HOMER Pro v3.16.2 was conducted by Ribó-Pérez et al. [16], which concerned the modeling of biomass gasifiers and hybrid renewable energy microgrids in rural communities in Honduras and Zambia. This study indicated that the hybrid system analyzed was technically and economically viable.

The research by Yew et al. [17] developed an optimal hybrid renewable energy system in HOMER Pro v3.16.2 software for Johor, Malaysia, integrating solar and biomass energy sources. The system, consisting of a 4075 kW PV, a 2100 kW biomass gasifier, 9363 battery units, and 1939 kW converters, proved to be cost-effective. It meets residential load demand with minimal unmet electric load and capacity shortage. This research highlights the economic viability and technical feasibility of a solar–biomass system.

An evaluation of the performance of a solar PV system combined with a biomass gasifier for electricity generation by Macías et al. [18] was carried out in Central and South America. The system consisted of a downdraft fixed-bed gasifier connected to a 30 kWe motor generator and a 5 kWe solar PV system, with a battery storage system.

The study by Xin et al. [19] introduced a biomass–solar hybrid system for sustainable fuel production, integrating solar-driven biomass gasification and PV electrolysis. The system improved energy efficiency by 6.57% and reduced the levelized cost of fuel by 12.5%. It also achieved a significant reduction in greenhouse gas (GHG) emissions, with an estimated -0.56 kg of CO_2 equivalent per kg of methanol produced.

In the studies referred to above, involving the hybrid systems of biomass gasification with PV systems, the common raw materials used are agro-industrial wastes such as sugarcane bagasse, eucalyptus, rice husks, palm kernel shells, coffee husks, pine needles, and rice straws, among others. However, there have been studies on the use of MSW in a hybrid PV system [20–22]. For example, Balan et al. [21], in a study carried out in Romania, made a techno-economic analysis of the on-grid hybrid system consisting of a 2.5 MW PV source and an MSW gasifier coupled to a 250 kWe internal combustion engine generator

set. PV production is prioritized in the system, operating from 8 a.m. to 4 p.m., and the MSW gasification generator acts as a backup only in situations where PV production is not available.

Sun and Tang [22] studied, in China, using Aspen Plus v11.0 software, an MSW gasification process integrated with solid oxide water electrolysis technology powered by PV panels to generate electricity and produce fuels such as methane, methanol, and dimethyl ether (DME). Pan et al. [20] carried out a similar study; however, the difference lies in the fact that theses authors focused on the technology for producing methane from the syngas generated, enriched by hydrogen (H_2) from water electrolysis.

Previous studies have explored some hybrid systems in diverse contexts, emphasizing their technical and economic viability. However, little research has been conducted on integrating MSW gasification and PV systems in developing regions like Lobito (Angola), where energy poverty and waste mismanagement are acute. To address this knowledge gap, this research seeks to answer the following research questions:

- How can the integration of MSW gasification and PV systems contribute to sustainable electricity generation in Lobito, Angola, a developing region?
- What are the technical, economic, and environmental impacts of implementing a hybrid MSW-PV energy system, including its feasibility in reducing energy poverty and improving waste management?
- Under what conditions can the hybrid system generate surplus electricity to support green hydrogen production through water electrolysis, and what are the key limitations in the current energy framework?

By addressing these questions, this research aims to explore the potential of combining a gasification plant of municipal solid waste (MSW) and a solar PV system to generate electricity and ensure a reliable power supply in Lobito, Angola. The primary objective is to evaluate the effectiveness of MSW gasification in electricity generation. Given that the current site for MSW landfilling has sufficient area and considering Lobito's potential for generating electricity through solar radiation, this study incorporates a PV system to evaluate the potential of the hybrid system (MSW gasification + PV system).

The electricity production from gasification is based on MSW arriving at the landfill, rather than waste already deposited (urban mining). The process involves generating syngas from the incoming MSW, which is then gasified on site. The resulting electricity is directly supplied to the grid, ensuring efficient local electric energy generation without the need to transport syngas to other locations. If a significant energy surplus is identified, the feasibility of producing green hydrogen (H_2) through water electrolysis is assessed. While this study includes an assessment of green hydrogen production via water electrolysis, it is recognized that this component's feasibility depends on the availability of electricity excess, which remains constrained in the current Lobito energy framework.

To achieve these aims, a modeling and simulation study was developed to evaluate the potential for electricity generation. For the PV system, data from PVGIS v5.3 [23], the PVsyst version 8 software, and MS Excel spreadsheets were utilized. A simulation of an MSW gasifier was conducted using Aspen Plus version 11.0. Both systems were integrated within the hybrid systems simulation software, HOMER Pro v3.16.2 version 3.16.2, incorporating an electrolyzer to assess the potential for green hydrogen generation from the electrical surplus of both systems.

This study is innovative, as there are currently no prior studies in the Lobito region and very few in Angola and Africa, making it a pioneering work in exploring the integration of MSW gasification and solar PV for electricity generation in this region. The novelty of this research lies in its comprehensive approach to modeling and simulating a grid-connected hybrid renewable energy system, which has not been previously attempted in Lobito. By

utilizing advanced simulation tools such as PVGIS v5.3, PVsyst v8, Aspen Plus v11.0, and HOMER Pro v3.16.2, this study provides a robust framework for evaluating the potential of hybrid renewable energy systems.

This research contributes to several key areas:

- Renewable energy integration: It advances the understanding of how MSW gasification and solar PV can be effectively combined to enhance energy security and reliability.
- Sustainable waste management: It offers insights into the use of MSW produced in Lobito as a valuable resource for energy production, promoting sustainable waste management practices.
- Environmental benefits: It aims to demonstrate the potential for a significant reduction in fossil CO_2 equivalent emissions through the adoption of renewable energy systems, contributing to global efforts to mitigate climate change.
- Green hydrogen production: By assessing the feasibility of green hydrogen generation from excess electrical energy, the research explores an innovative pathway for hydrogen economy development.

Furthermore, this research provides practical implications for local authorities and policymakers by showcasing the potential benefits of implementing hybrid renewable energy systems in urban areas. The findings of this study could serve as a reference for future energy planning initiatives, encouraging the inclusion of innovative energy recovery projects from MSW in developing countries.

2. Methodology

Figure 2 presents a flowchart illustrating the key methodological steps followed in this study.

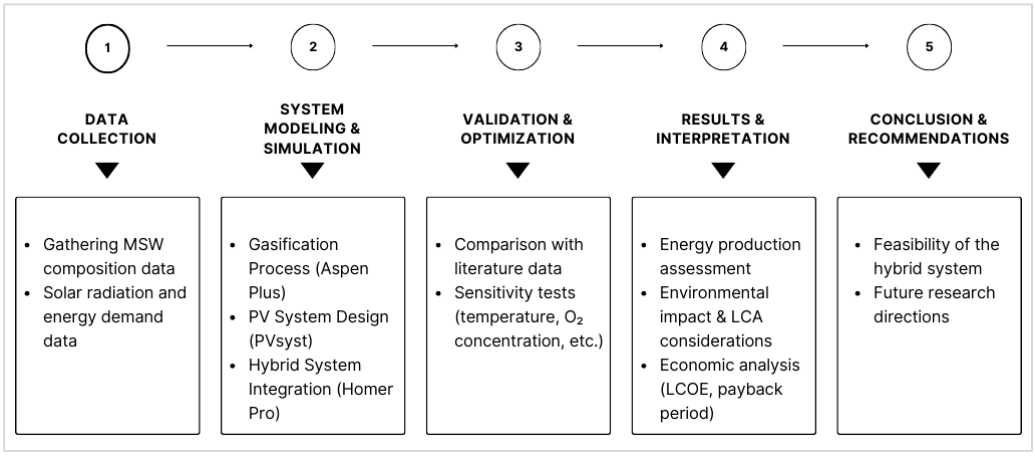

Figure 2. Methodological flowchart.

The methodology includes data collection on MSW composition and solar energy potential, system modeling and simulation using specialized software, validation and optimization processes, and the final analysis of results. This structured workflow ensures a comprehensive evaluation of the feasibility of the hybrid system.

2.1. Modeling and Simulation of an MSW Gasification Unit

Gasification is a thermochemical process that converts organic materials, such as MSW, into a combustible gas mixture, called syngas, under the controlled conditions of temperature and oxygen [24–26]. The primary reactions include the following:

1. Pyrolysis: The thermal decomposition of waste in the absence of oxygen, producing char, tar, and volatile gases.
2. Combustion: The partial oxidation of carbon-based materials to generate heat for sustaining the process (e.g., $C + 0.5\ O_2 \rightarrow CO$; $\Delta H = -111$ MJ/kmol).
3. Reduction: The conversion of CO_2 and water vapor into CO and H_2 via reactions such as the water–gas shift ($CO + H_2O \rightarrow CO_2 + H_2$; $\Delta H = -41$ MJ/kmol) and the Boudouard reaction ($C + CO_2 \rightarrow 2\ CO$; $\Delta H = +172$ MJ/kmol).

For the success of modeling the process flowchart on Aspen Plus v11.0, it was necessary to rely mainly on the models used by Begum et al. [27] and Moshi et al. [28]. Their studies only provide generic and contextual data; therefore, it was necessary to survey the Lobito Municipal Administration to obtain specific information related to MSW. As this government body does not have some data, it was necessary to resort to bibliographic data provided by the World Bank and the African Development Bank and studies on waste composition in similar contexts.

Considering the total number of residents currently estimated in Lobito is at 484,351 inhabitants, a total amount of around 200 t/day (wet weight) of MSW generated is estimated at a conservative production rate of 0.41 kg/(day.inhabitant). Thus, the processing capacity of the gasification system sized in this study was 200 t/day (wet weight) with an average water content of 39.47%.

According to the World Bank, Angola falls into the group of lower-middle-income countries. Using the data provided by Dong [29] and Hadi [30] regarding the typical percentage of materials present in MSW, it was possible to establish an average composition of MSW in the city of Lobito (Table 2).

Table 2. Estimated proximate analysis of MSW from Lobito.

Proximate Analysis	Wt%
Moisture	39.47
Fixed carbon	6.45
Volatile matter	13.95
Ashes	40.13

The elemental composition of the MSW from the city of Lobito was estimated as having the values shown in Table 3.

Table 3. Estimated elemental composition of MSW from Lobito (values expressed as % of dry matter).

Chemical Element	Wt%
Carbon	33.97
Hydrogen	4.27
Nitrogen	1.14
Chlorine	0.02
Sulfur	0.14
Oxygen	20.33
Ashes	40.13

Proximate analysis (Table 2) was inserted into the Phyllis online database [31], from which the low heating value (LHV) of Lobito's MSW was automatically calculated as 7.82 MJ/kg. While this value exceeds typical LHVs reported for MSW in other cities in developing countries, it reflects the relatively low fraction of organic waste and the high proportion of non-biodegradable materials such as plastics and textiles in Lobito's MSW. It is recommended that future research studies include additional local surveys and waste

characterization campaigns to further refine these estimates and improve their statistical robustness and repeatability, as the Phyllis online database is mainly a European database, probably not applicable to Angola's reality.

The gasifier modeled in this study is a fixed-bed downdraft gasifier due to its advantages in handling MSW with varying moisture and ash contents. However, it is important to note that this selection serves as a reference for analysis and does not imply that it is the only viable gasification technology. Depending on specific implementation conditions, other configurations such as fluidized-bed gasifiers may offer operational advantages, particularly in terms of mixing efficiency and adaptability to heterogeneous waste compositions.

The key operating parameters were modeled, including the equivalence ratio (ER), gasification temperature, MSW flow rate, and air flow rate. The ER used was 0.1, and the injection and proper distribution of air within the system were managed through a FORTRAN statement defined in the calculator (C-2) of the Aspen Plus v11.0 flowchart.

It is important to note that in calculator C-2, the equation aimed to determine the mass flow rate of the feedstock stream by accounting for its pure and non-conventional components while subtracting the mass flow rates of O_2 and N_2 already present in the stream. Since both are components of air, this adjustment ensured a properly balanced air supply. Equation (1) was used:

$$\dot{m}_{ag} = ER \times \left(\frac{\dot{m}_{feed}}{X_{O_2}} - \dot{m}_{O_2} - \dot{m}_{N_2} \right) \quad (1)$$

where

$\dot{m}_{ag}$—the mass flow rate of the gasifying agent injected into the system (kg/h).
$\dot{m}_{feed}$—the total mass flow rate of the feedstock stream (kg/h).
X_{O_2}—the mass fraction of O_2 in the gasifying agent, which can vary between 0.21 and 1.
$\dot{m}_{O_2}$—the mass flow rate of O_2 present in the feedstock stream (kg/h).
$\dot{m}_{N_2}$—the mass flow rate of N_2 present in the feedstock stream (kg/h).
ER—the equivalence ratio, ranging from 0.1 (partial oxidation) to values greater than 1 (complete oxidation).

To ensure downstream applications, the syngas underwent preliminary treatment to remove ash (cyclones) and tar (condensation). The advanced removal of contaminants like HCl and H_2S, though beyond this study's scope, was discussed as essential for long-term system viability and syngas quality. Key outputs included syngas composition, LHV, Cold Gas Efficiency (CGE), and Carbon Conversion Efficiency (CCE). The syngas composition, dominated by CO, H_2, and CH_4, was validated against bibliographic data, ensuring the model's reliability.

The proposed model for the MSW gasification system is shown in the simplified block diagram in Figure 3 and detailed in the process flowchart in Figure 4. Much of the data used for modeling purposes in Aspen Plus v11.0 was mainly obtained from the available literature [27,28].

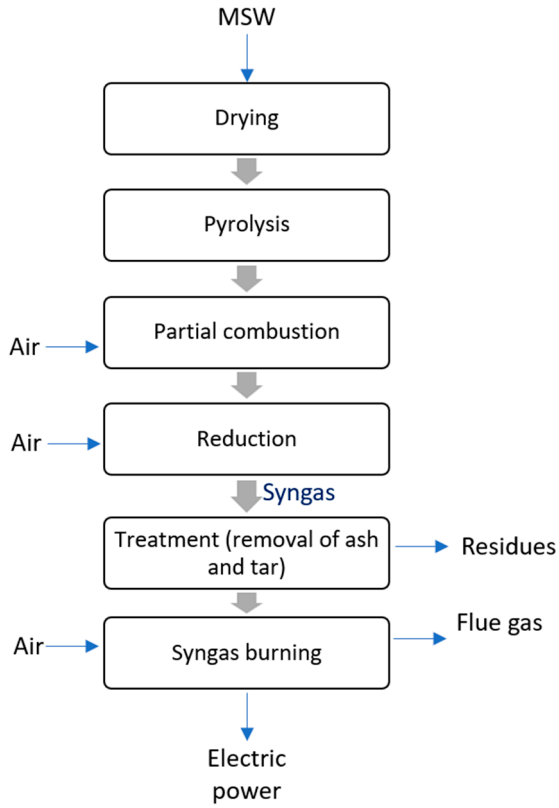

Figure 3. Simplified process diagram of the gasification system with electricity generation.

The model was developed under the following assumptions:

- The process runs in a steady-state condition.
- The combustion and reduction blocks are isothermal.
- Char is assumed to consist of carbon and ash.
- Ash does not participate in the chemical reactions as it is considered inert.
- All the sulfur is converted into H_2S.
- All the chlorine is converted into HCl.
- No nitrogen oxide is formed, but only NH_3 is produced; however, its content is so low that it does not cause significant inaccuracies in the simulation.

The flowchart shown in Figure 4 illustrates the MSW gasification and subsequent electricity generation. It is structured into several sections to depict each stage of the process:

1. Drying: This stage removes moisture from the waste material using a dryer and a drying drum, operating at temperatures up to 120 °C.
2. Pyrolysis: The dried waste undergoes thermal decomposition in the absence of oxygen in a pyrolysis reactor at a temperature of 650 °C, producing pyrolysis gas.
3. Gasification: The pyrolysis gas and remaining waste are converted into syngas (a mixture of H_2 and CO), with the assistance of an air compressor, with gasification occurring at up to 750 °C.
4. Syngas treatment: The syngas is cleaned and conditioned to remove impurities like ash and tar using components such as cyclones and separators.
5. Power Recovery Unit 1: The cleaned syngas is used to generate electricity through a gas turbine, connected to a power generator.
6. Power Recovery Unit 2: Waste heat from the gas turbine is used to generate additional electricity through a vapor turbine, connected to another power generator.

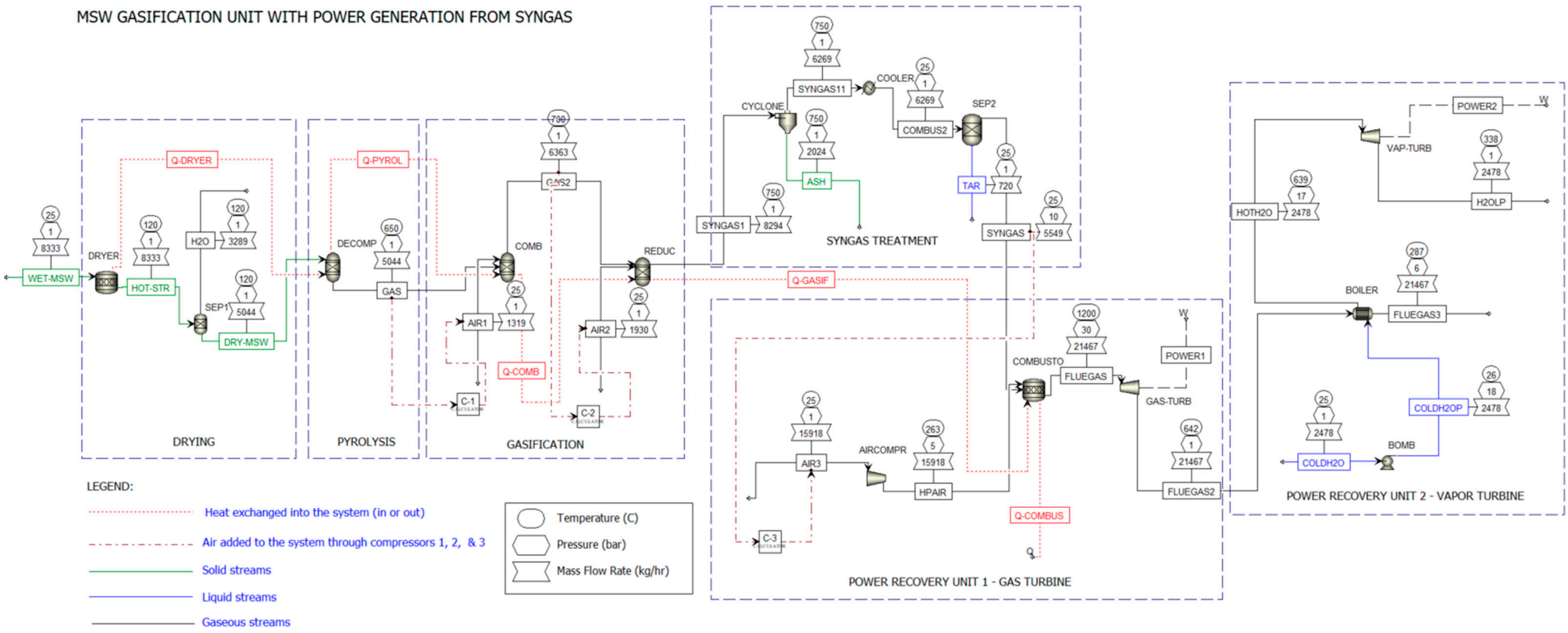

Figure 4. Flowchart of the MSW gasification process modeled in Aspen Plus v11.0 (C-1 calculator; C-2 calculator; C-3 calculator).

2.2. Modeling and Simulation of a Photovoltaic Solar Power Plant

The solar PV system design and energy yield were analyzed using local solar radiation data, panel specifications, and shading simulations. The PVsyst v8 software provided detailed reports on the performance ratio (PR), energy losses, and environmental benefits (e.g., reduction in CO_2 equivalent emissions).

Since the intention is to model a hybrid system, the PV system is proposed to be installed in the vicinity of the Lobito dump (12°23′39.53″ S; 13°38′11.92″ E), which, according to the Google Earth simulation, currently has a perimeter of approximately 2 km and an area of approximately 15 hectares (Figure 5). Therefore, by installing the gasification plant to process the majority of the MSW and considerably reducing the need for additional landfill space, this study proposes allocating 5 hectares for the solar PV installation.

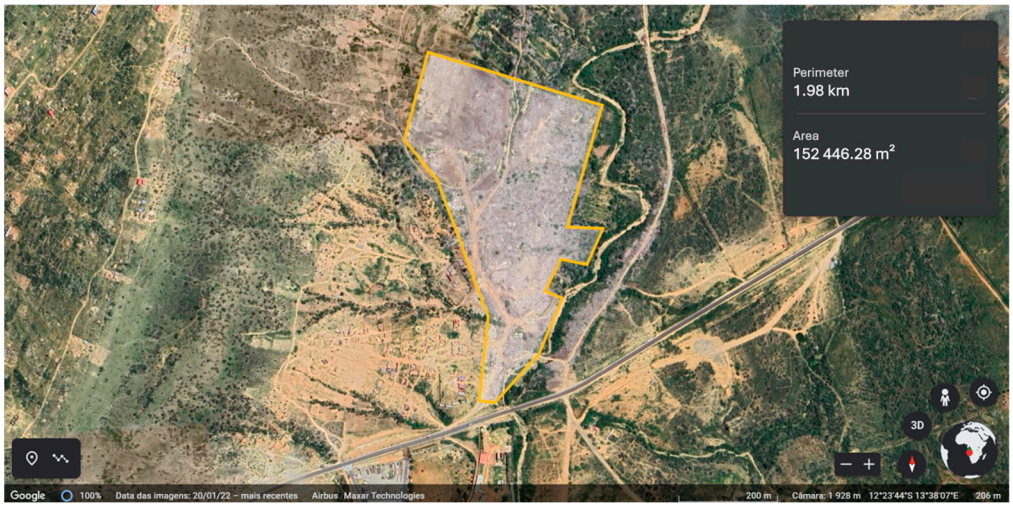

Figure 5. Current MSW disposal zone in the Lobito landfill.

Since Lobito is located in the Southern Hemisphere, the PV panels will have to be oriented in the Northern direction. The optimum angle and azimuth positions were analyzed using the European Commission's PVGIS v5.3 database [23]. PVGIS recommends an optimum angle of 15° and an azimuth of −179° (−1° in PVsyst v8). Since the site where the system will be installed does not have an azimuth of 180° (0° in PVsyst v8), the panels will have to be installed according to the layout of the field. Therefore, the optimum angle of 15° was maintained when configuring the system in PVsyst v8, and the azimuth was set to −20° (−160° in PVGIS v5.3).

The PV module with the highest peak power currently available was chosen—model UP-M670MH-66G12—made of monocrystalline silicon by Upsolar (Shanghai, China), manufactured in 2021, with a peak power of 670 Wp. Table 4 shows some of the data available on the manufacturer's datasheet.

The inverter for the installation was selected based on the criterion outlined in Equation (2):

$$70\% \times P_{inst} < P_{invert} < 120\% \times P_{inst} \quad (2)$$

where P_{inst} is the power peak of the installation and P_{invert} is the nominal inverter power. Therefore, the Sungrow's inverter model SG2500-HV-20 (production in Hefei, Anhui, China; headquarters in Costa Mesa, CA, USA) was selected, with 2500 kW of nominal AC output power. Table 5 shows the main data of the selected inverter, according to its respective datasheet. Since the installation of the PV system was considered in the same location as the MSW gasification plant, its layout and possible shadowing effects were simulated in PVsyst v8 and SketchUp v2023.0 software by building the 3D scenario. The structure, with

an approximate area of 3 hectares for a 200 t/day capacity MSW plant, was oriented to the South, opposite the PV module faces, to prevent shading (Figure 6).

Table 4. Features of the UP-M670MH PV module.

Parameter	Value
Peak power	670 Wp
Voltage at maximum power, VMPP	38.15 V
Current at maximum power, IMPP	17.562 A
Open-circuit voltage, VOC	45.85 V
NOCT	45 °C
Short-circuit current, ISC	18.600 A
Maximum acceptable temperature	90 °C
Minimum acceptable temperature	−40 °C
Maximum efficiency	21.57%
Length	2.384 m
Width	1.303 m
Coefficient of power (αp)	−0.34%
No-load stress coefficient (αVoc)	−0.25%
Short-circuit current coefficient (αIsc)	0.040%

Table 5. Features of the SG2500-HV-20 inverter.

Parameter	Value
Rated and maximum AC power	2500 kW and 2750 kW
Maximum efficiency	99%
$U_{min.}$ MPP	800 V
$U_{max.}$ MPP	1300 V
$U_{max.\ inv.}$	1500 V
I_{MPP}	3508 A
Weight	6500 kg
Length × Width × Height	2591 m × 2438 m × 2991 m

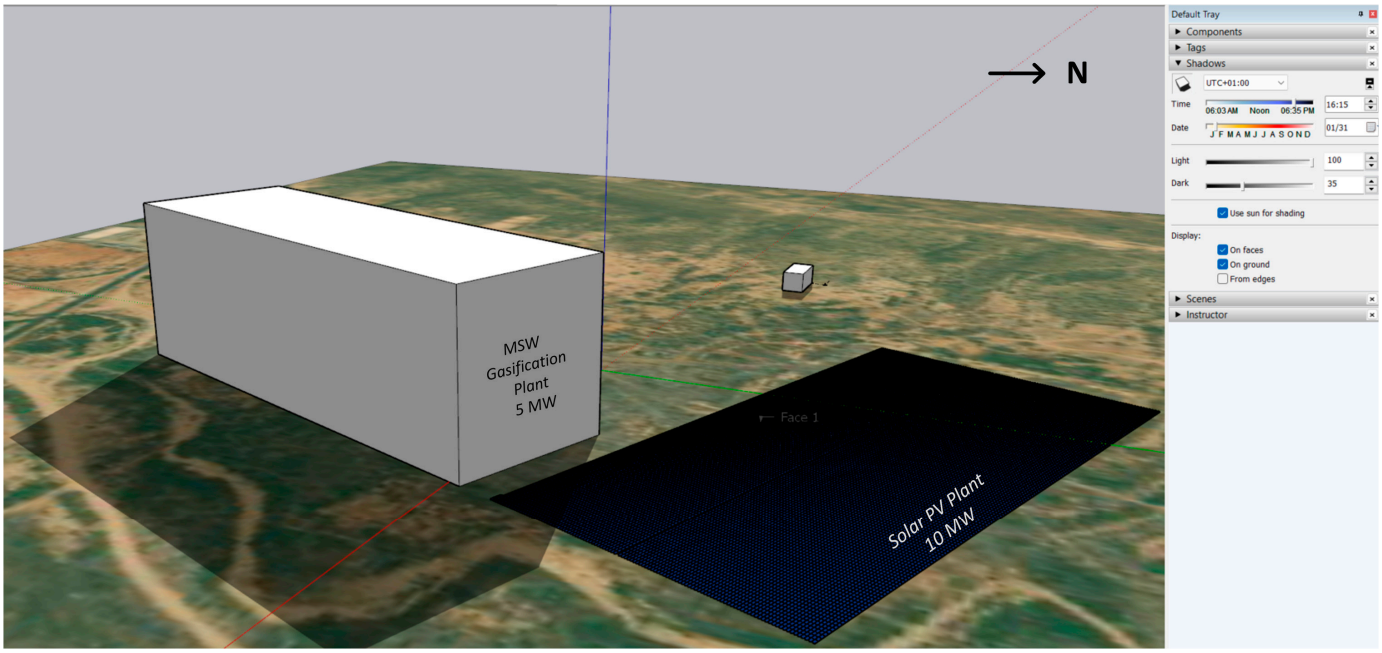

Figure 6. Simulating shading in SketchUp v2023.0 software.

2.3. Simulation of System Integration: MSW Gasification, Solar PV Plant, Water Electrolysis, and Public Electricity Grid

The integration of the systems was analyzed through modeling and simulation in the HOMER Pro v3.16.2 software. The hybrid system was modeled by inserting (a) an electrical grid component, (b) a syngas generator producing the same electrical power obtained in the Aspen Plus v11.0 simulation, (c) a solar PV system with the same peak power as that obtained in the PVsyst v8 sizing, (d) a water electrolyzer, (e) a hydrogen tank, and (f) a fuel cell, in a system with a load that was calculated to have a peak power demand of approximately 770 MW, corresponding to the Lobito region. Figure 7 summarizes the hybrid system modeled in HOMER Pro v3.16.2.

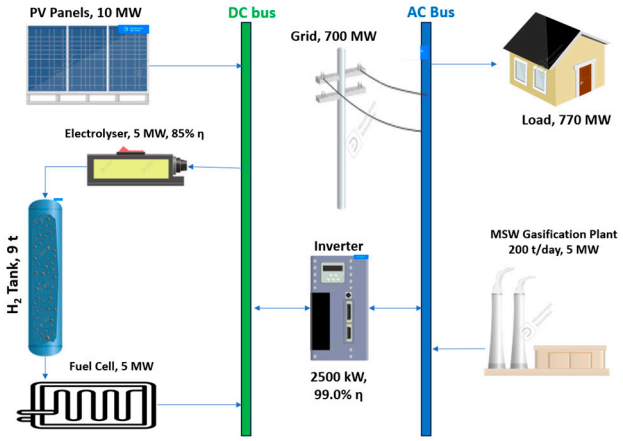

Figure 7. Hybrid system simulated in HOMER Pro v3.16.2.

The water electrolysis system was included in the hybrid model, in HOMER Pro v3.16.2, to assess its potential under the hypothetical scenarios of electricity surplus. However, given the current deficit in electricity supply in the region, the practicality of this component remains limited and contingent on future production capacity expansions.

Rather than representing an existing commercially available unit, the model incorporates typical electrolysis parameters, including efficiency, the hydrogen production rate, and operational constraints, based on industry data.

This approach allows for an optimized simulation of the system's performance without relying on a specific supplier or custom-built prototype. Future studies may explore commercially available electrolysis systems to validate the assumptions made in this model.

Metrics such as LCOE, electricity production (GWh/year), and payback period (years) were calculated and generated in HOMER Pro v3.16.2. The model incorporated hourly load data for the Lobito region to assess grid reliability and penetration rates.

A 5 MW gasifier was designed to process 200 t/day of MSW, producing syngas with a lower heating value (LHV) of 8.69 MJ/kg. Operating continuously for 24 h, the gasification unit compensates for the intermittency of solar PV, ensuring a steady power supply. This hybrid approach underscores the essential role of gasification in renewable energy systems, especially in areas prone to energy shortages.

The solar PV system was configured based on the information made available throughout the study on PVsyst v8.

An electrolyzer with a capacity of 5 MW was configured, with 85% efficiency and DC output. The hydrogen produced was sent to a 9 t storage tank, with no initial rate of stored hydrogen. The fuel cell configured had a maximum output of 5 MW, with a DC electrical bus that produces electrical energy from stored hydrogen. The thermal energy generated was not considered.

Finally, the public electricity grid—modeled with a variable load of 500–700 MW—was analyzed to assess its response to the integration of the hybrid renewable energy system and the associated load-response dynamics.

Regarding the peak power demand of 770 MW, it is important to explain how this value was calculated. According to JICA et al. [32], in a report on the electric sector development project in Angola until 2040, the central region—where the study region is located—is expected to have a peak power demand of 877 MW for residential, commercial, and industrial customers by 2025, considering the current electrification rate. The maximum demand per consumer is estimated to be 1.589 kW for the studied region. Without considering the electrification rate, assuming a general demand based on the current number of residents in Lobito (484,351 inhabitants) and the per capita demand rate of 1.589 kW, the general demand power was calculated as 770 MW.

Based on the information presented and the load diagrams proposed by JICA et al. [32], it became possible to define the specific load diagram for the study region (Figure 8), whose data was then used to configure the public electricity grid in HOMER Pro v3.16.2 software.

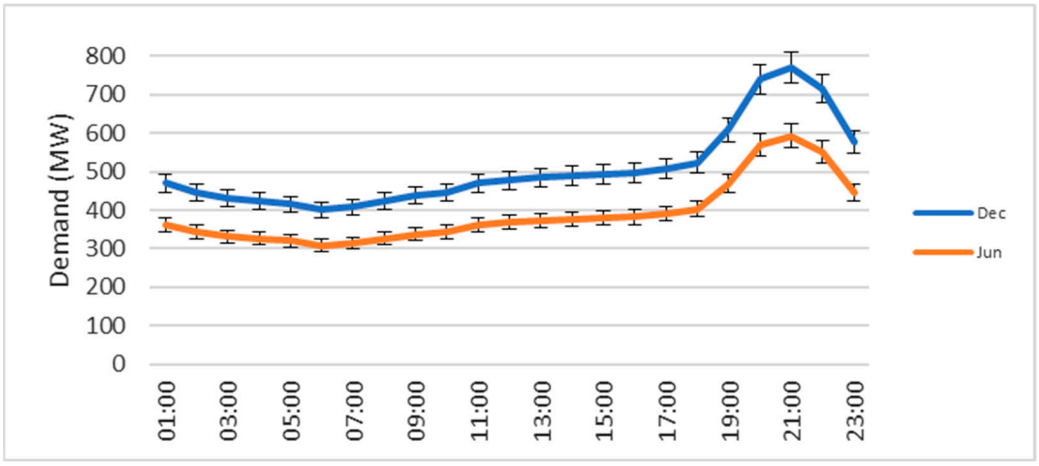

Figure 8. Load diagram by the number of residents in the study region.

3. Results and Discussion

3.1. MSW Gasification Performance

The model created in Aspen Plus v11.0 was validated through a sensitivity study to evaluate the system's behavior and compare it with experimental data reported by different authors. Additionally, the study carried out by Begum et al. [27], which is part of a numerical investigation into the gasification of MSW using Aspen Plus v11.0, was considered for the specific validation of the model of the present study. The same input data was used, and the results were compared. The data from Begum et al. is described in Tables 6 and 7.

Table 6. Characteristics of MSW used in the study by Begum et al. [27].

Proximate Analysis (Wt%)		Ultimate Analysis (Wt%)	
Moisture	12	Carbon	36.4
Fixed carbon	15.47	Hydrogen	4.97
Volatile matter	38.29	Oxygen	10.15
Ashes	46.24	Sulfur	0.80

Comparing the results obtained in this work with those of Begum et al.'s study [27], the model in this study proved to be viable for simulating the gasification of MSW. This viability

ensures the projection of the gasifier's performance under different operating conditions. Similarly to Begum et al.'s study, the model's validation showed that as the ER increases from 0.1 to 1 and the gasifier temperature is maintained at 700 °C, the concentration of CO decreases from 70% to 40%, H_2 decreases from 14% to 3%, CO_2 increases from 17% to 58%, and CH_4 decreases from 6% to zero and stabilizes (Figure 9). In Begum et al.'s study [27], CO decreased from 75% to 40%, H_2 decreased from 10% to 2%, CH_4 did not vary, and CO_2 increased from 10% to 40%.

Table 7. Operating parameters of the gasifier used in the study by Begum et al. [27].

Parameter	Feed	Air	Gasifier
Mass flow (kg/h)	10	1–10	-
Pressure (bar)	1	1	1
Temperature (°C)	25	25	500–1000

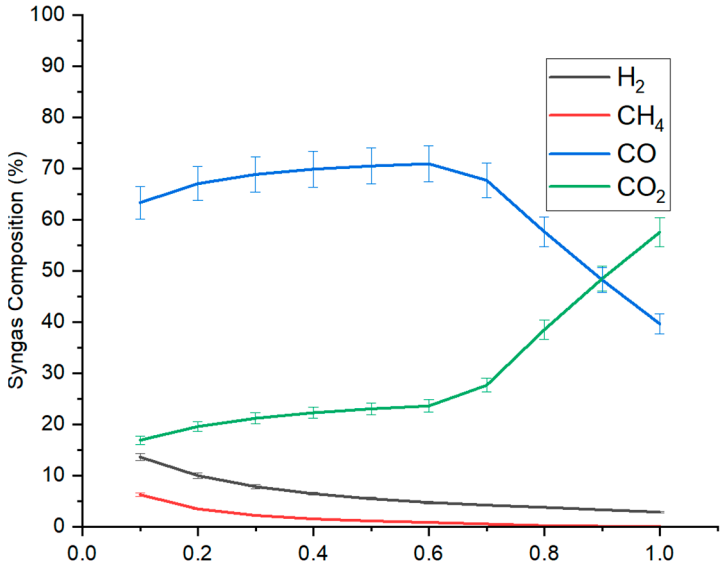

Figure 9. Model validation of MSW gasification: variation in syngas composition as a function of ER.

This relative difference in composition is because the model in this study includes more substances in the product, namely, SO_2, SO_3, NO_2, NO, and NH_3, in addition to those considered by Begum et al. [27].

3.1.1. Sensitivity Analysis: Effect of ER Variation

The gasifying agent used in this study was air. The air quantity was changed in the gasifier's reduction section (COMBUST block of the Aspen Plus v11.0) between the ER values of 0.1 and 1, with a variation step of 0.1, resulting in ten analysis points; 0.1 of air corresponds to 1930 kg/h of air, with a relative O_2 concentration of 0.21 (21% *v*/*v*). Figure 10 shows the results of the effects of varying the air under the same operating conditions of temperature and pressure.

The variation in ER promotes gasification reactions that produce high levels of CO and H_2. For ER values above 0.3, this process is reversed, with complete oxidation reactions being intensively promoted, namely, CO, H_2, and CH_4 oxidation reactions, resulting in an accelerated increase in CO_2 and H_2O concentrations and a decrease in CO, H_2, and CH_4 concentrations. Under stoichiometric air conditions (ER = 1) or excess air (ER > 1), the CO and H_2 contents tend towards zero, with CH_4 being oxidized long before the stoichiometric ER condition.

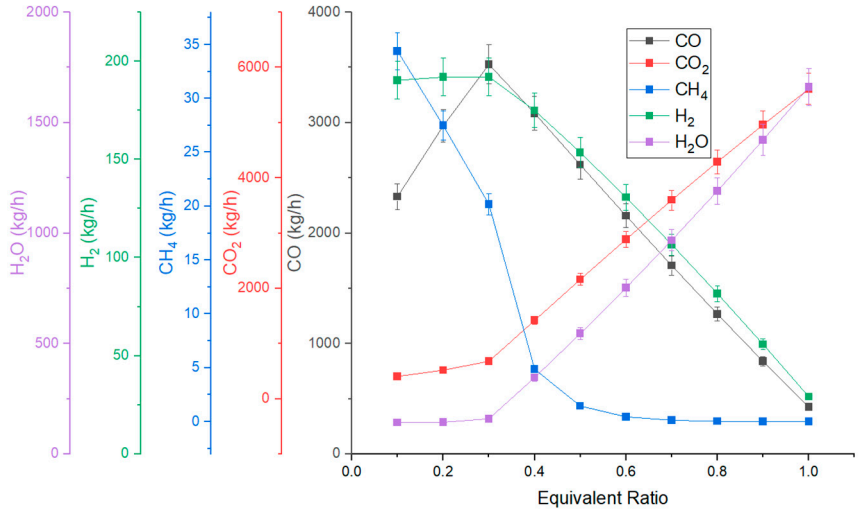

Figure 10. Effects of ER variation on syngas composition.

The behavior of LHV, CGE, and CCE is shown in Figure 11. For ER values of 0.1 to 1, the LHV decreases since the considerable increase in air leads to an increase in the concentrations of H_2O and CO_2, as well as an increase in N_2, and a decrease in the concentrations of CO, H_2, and CH_4.

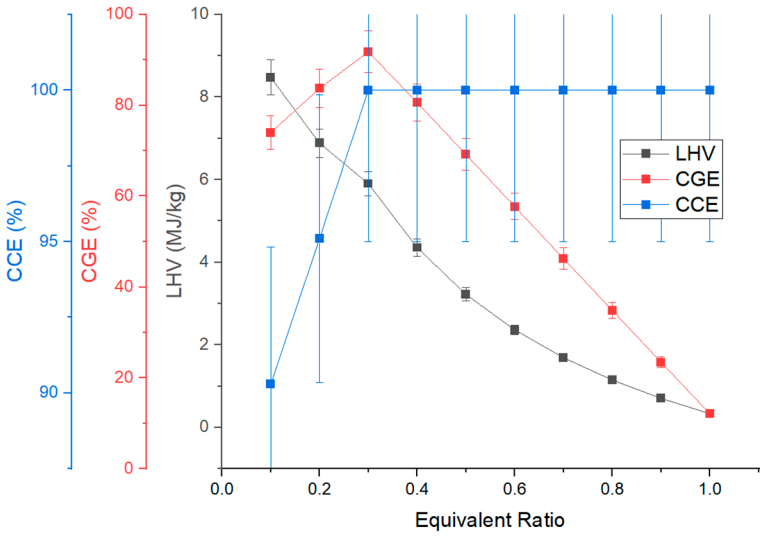

Figure 11. Effects of ER variation on LHV, CGE, and CCE.

The CCE increases for ER values of 0.1 to 0.3 and then stabilizes. For ER values below 0.3, there is a remaining amount of tar in the system, which means that not all the carbon has been converted into syngas. For ER values above 0.3, all the carbon compounds previously present in the raw material are converted into other compounds. Although this ER was not used as a standard in this study, it can be concluded that an ER value of 0.3 is ideal for avoiding the formation of tar.

Concerning CGE, a ratio that corresponds to the ability to extract the maximum amount of energy from the syngas produced during gasification, up to an ER of 0.3, there is no excess oxidation, as mentioned above. In other words, by increasing the content of the main energy components of syngas—CO, H_2, and CH_4—the CGE value increases. However, for ER values above 0.3, the oxidation of the gases with energy content in syngas occurs, causing a gradual decrease in CGE as the ER increases.

3.1.2. Sensitivity Analysis: Effect of Temperature Variation

A sensitivity analysis was conducted to evaluate the effects of temperature variation in the gasifier, ranging from 50 to 1000 °C. This temperature range was selected to cover both low- and high-temperature regimes, providing a comprehensive understanding of the thermochemical conversion of MSW into syngas. This variation was applied in the reduction section of the gasifier, identified as the COMBUST block, with a step increment of 50 °C, resulting in 20 points. In this section, the impact of temperature variation on syngas yield, its composition, and key performance parameters, including LHV, CGE, and CCE, is examined. The results are presented in Figures 12 and 13.

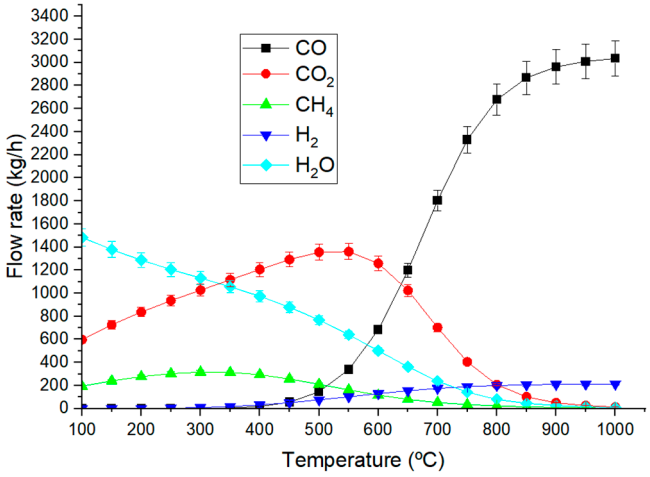

Figure 12. Effects of temperature variation on syngas composition.

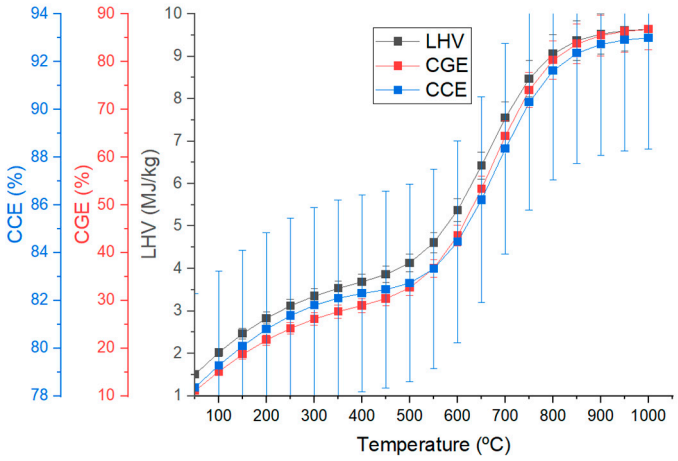

Figure 13. Effects of temperature variation on LHV, CGE, and CCE.

As observed in Figure 12, at an ER of 0.1, favorable for gasification reactions, exothermic reactions occur predominantly at temperatures below approximately 500 °C. These reactions include the incomplete oxidation of char, where the formed CO reacts with excess H_2O via the water–gas shift reaction, producing CO_2 and H_2. The resulting H_2 can further react with char or additional CO through hydrogenation or methanation, respectively, leading to CH_4 formation. This explains the significant presence of CO_2 and CH_4 at lower gasifier operating temperatures (<500 °C).

As the temperature increases beyond 500 °C, the formation of syngas components shifts due to the equilibrium of chemical reactions, favoring endothermic processes such as the Boudouard reaction, the water–gas reaction, and methane steam reforming, resulting in increased CO and H_2 production.

The upper limit of 1000 °C was chosen to ensure that the analysis captures the transition between different reaction pathways and determines the optimal temperature range for syngas generation, even if the higher temperatures are not very common in gasification technologies.

As observed in Figure 13, the temperature variation leads to an increase in LHV as gasification reactions progress, promoting the formation of the primary energy-carrying syngas components, namely CO and H_2.

Regarding CGE, the same principle applies; since the process transitions from a state where char is not converted into syngas to a state where syngas components are actively generated, without excess oxidation, the CGE gradually increases. Higher temperatures (up to 1000 °C) enhance syngas quality by minimizing tar formation and improving CGE, which is critical for downstream energy conversion [27,28].

For CCE, the gradual increase in temperature enhances the efficient conversion of solid carbon into high-energy gaseous products, thereby improving overall system performance.

3.1.3. Sensitivity Analysis: Effect of Varying O_2 Concentration on the Injected Gasifying Agent

At standard atmospheric conditions, O_2 is present at a concentration of 21% (*v/v*), mixed with 78% (*v/v*) N_2 and approximately 1% (*v/v*) of other gases. In this study, atmospheric air was assumed to contain only O_2 and N_2, at concentrations of 21 and 79% (*v/v*), respectively. Based on this assumption, an evaluation was conducted on the effect of varying the O_2 concentration in the injected gasifying agent, i.e., the impact of O_2 enrichment on the gasification process. The analyzed concentrations were 21, 40, 60, 80, and 100% (*v/v*), under constant pressure and ER conditions.

Since an increase in O_2 concentration naturally enhances the oxidation reaction rate for exothermic reactions, leading to a rise in system temperature, this analysis incorporated a temperature variation of 20 °C for each O_2 increment, up to 100% (*v/v*) O_2 in the gasifying agent. Figure 14 illustrates the effects of this variation on LHV, CGE, and CCE.

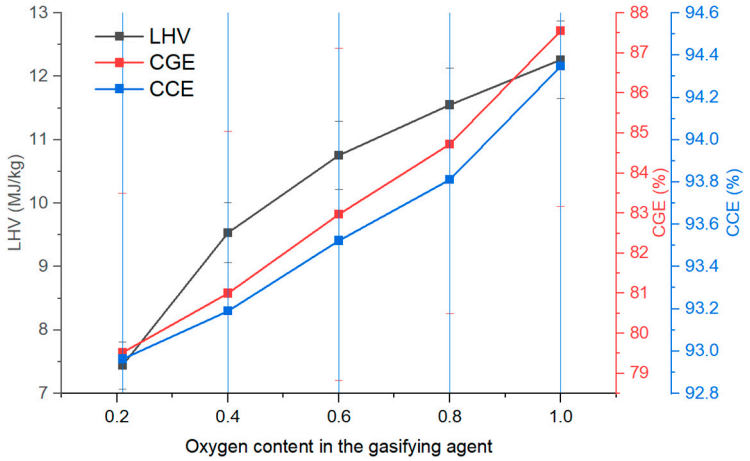

Figure 14. Effects of oxygen content variation in the gasifying agent on LHV, CGE, and CCE.

To better interpret these results, it is essential to consider Equation (1), which defines the mass flow rate of the injected gasifying agent. For a fixed ER value of 0.1, increasing the O_2 concentration in Equation (1) results in a reduction in the mass flow rate of the gasifying agent due to the proportional decrease in N_2 content. The absence of inert substances in the syngas significantly increases its LHV, as confirmed by the trend observed in Figure 14. Furthermore, increasing the purity of the gasifying agent enhances the availability of O_2 for reactions with carbonaceous material, accelerating partial oxidation reactions and

consequently improving the CCE. This also favors CO and H_2 production, leading to higher CGE. Additionally, the reduction in the formation of undesirable byproducts, such as tar, enhances process efficiency and minimizes the need for extensive syngas treatment.

3.1.4. Syngas Treatment

The syngas generated in the MSW gasification plant can contain contaminants such as ash, tar, HCl, H_2S, and NH_3, necessitating treatment before its final use to avoid compromising downstream processes and to mitigate harmful effects on human health and the environment. In the Aspen Plus v11.0 model created for this study, the syngas was only treated for ash removal using cyclones and for tar removal through condensation and physical separation (Figure 15). Therefore, the model does not include treatment units for the removal of HCl, H_2S, and NH_3, as this was not the focus of the study. However, it is important to mention additional syngas treatment methods for removing these contaminants, as described below.

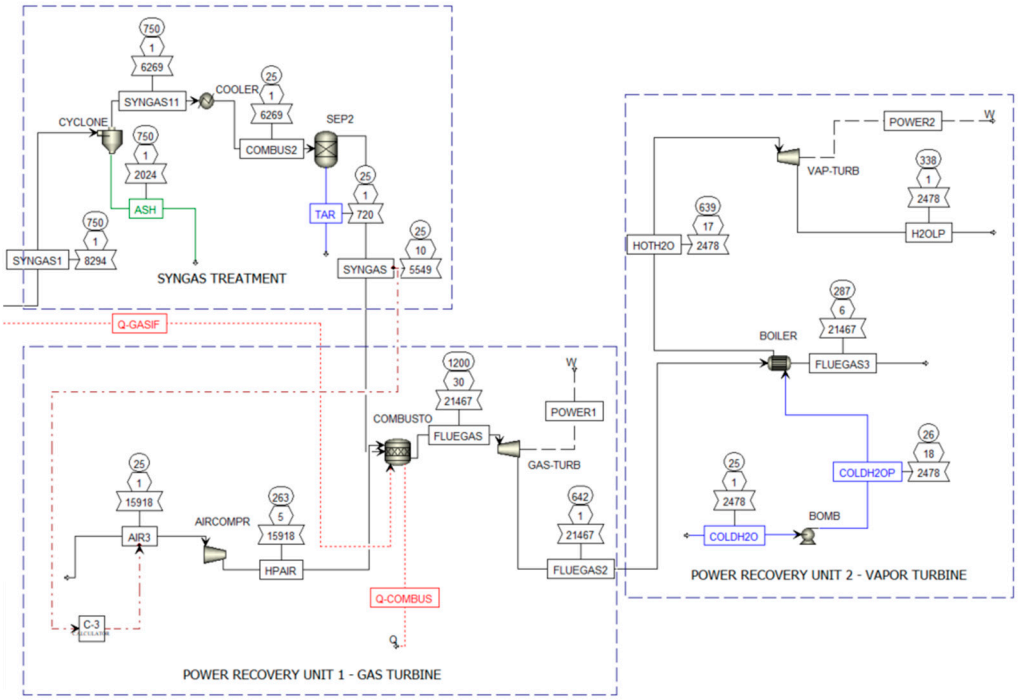

Figure 15. Syngas treatment and electric power generation units modelled on Aspen Plus v11.0 (C-3: calculator).

Due to the harmful effects of NH_3 on human health and the environment, as well as its potential to negatively interfere with subsequent syngas conversion or utilization processes, typical treatment processes include water scrubbers, adsorption with activated carbon or zeolites, and catalytic conversion, which can convert NH_3 into molecular N_2 [33].

H_2S poses a significant challenge to any process due to its toxic and corrosive nature, presenting risks to human health and the environment. Typical treatments include the following: (a) chemical adsorption, such as washing with a specific solvent, usually an amine solution, which reacts with H_2S to form ammonium salts; (b) physical adsorption using activated carbon impregnated with zinc; and (c) catalytic oxidation (Claus process), which promotes the formation of elemental sulfur, subsequently collected from the system [33,34].

HCl is an extremely corrosive and toxic gas, posing risks to human health and the environment. The main treatments for syngas include the following: (a) alkaline washing, typically with sodium hydroxide (NaOH) or potassium hydroxide (KOH), forming sodium chloride (NaCl) or potassium chloride (KCl), respectively; (b) adsorption with modified

zeolites or alkaline carbonates, forming alkaline salts; and (c) catalytic reaction, converting HCl into molecular chlorine through a reaction with oxygen or into chlorosulfonic acid (HSO_3Cl) through a reaction with sulfur dioxide, which are less toxic products that can be further treated by appropriate methods [33].

3.1.5. Power Generation from Syngas

The power generation unit selected for the gasification system was of the combined cycle type, consisting of a gas turbine and a steam turbine. The gas turbine generates power from the combustion of syngas, while the residual heat is utilized in a steam cycle to produce additional electricity, improving the overall system performance. After expansion in the gas turbine, the combustion gases go to a boiler to generate water vapor, which in turn goes to a steam turbine to generate electricity (Figure 15).

This system generates 4.81 MW of power, with the gas turbine generating approximately 4.37 MW and the steam turbine generating approximately 0.44 MW.

Notably, parameters such as the syngas LHV, flue gas pressure, and temperature can be altered by the operation of the gasifier and have a direct influence on the electrical power that the system can generate.

3.1.6. GHG Savings in the Gasification System

The GHG emissions savings in the gasification system were estimated using Equation (3), as presented below:

$$MSW\ gasification\ CO_2\ balance = E_{grid} \times E_{f-diesel} \quad (3)$$

where

MSW gasification CO_2 balance—the total amount of CO_2 emissions avoided by replacing grid-supplied electricity with MSW gasification-generated electricity (t CO_2).
E_{grid}—annual electricity generation from the MSW gasification system that would otherwise be drawn from a diesel-powered grid (MWh).
$E_{f\text{-}diesel}$—CO_2 emission factor related to diesel engines (kg CO_2/kWh).

The MSW gasification unit in this study generates approximately 42 GWh/year of electricity. Assuming that this electricity would otherwise be produced using diesel generators (common in Angola), with an average emission factor of around 1.0 kg CO_2/kWh [35,36], the estimated annual amount of CO_2 emissions avoided is approximately 42,000 tons. This value aligns with standard assumptions that syngas emissions from biogenic waste are considered carbon-neutral under IPCC guidelines [35]. These findings highlight the substantial climate benefits of displacing diesel-based generation through MSW gasification, particularly in regions like Angola, where fossil fuels remain an important primary energy source for electric energy production [37,38].

3.2. PV Production

3.2.1. Analysis of Relevant System Parameters

For the defined area of 5 hectares and based on the type of module defined (UP-M670MH), 16,095 modules were considered to be horizontally installed, occupying a total area of 4.9 hectares, generating a peak DC power of 10.784 MWp (Figure 16), for an AC output power of 10 MW.

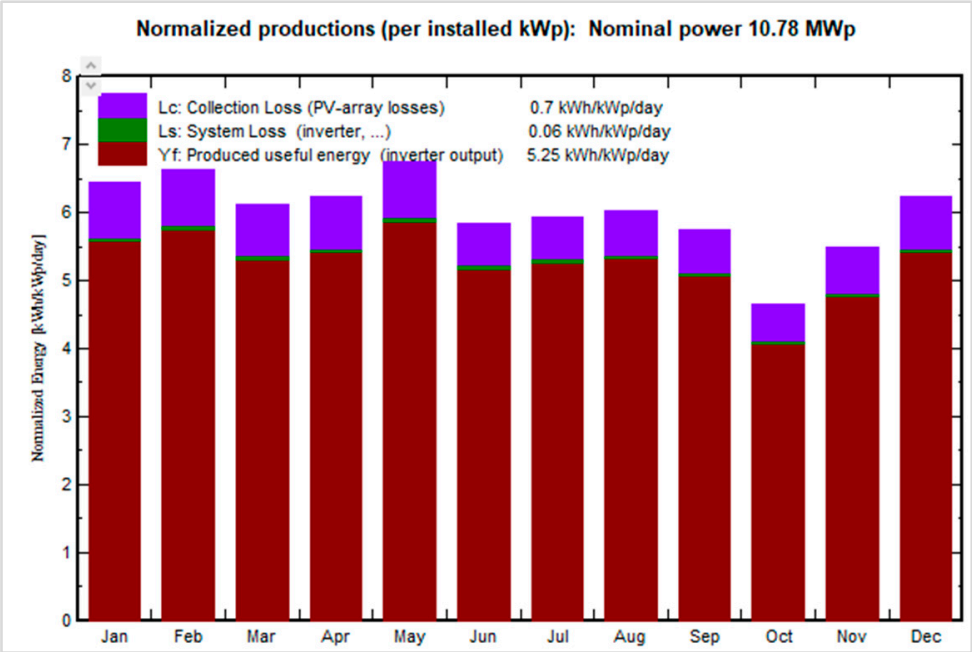

Figure 16. Monthly PV system production.

The system has a performance index of 87%, indicating a considerable amount of electricity generated compared to the energy that would be produced under STC conditions. Low-performance index values represent the possible poor inclination of the PV modules, the presence of shading, or even losses in the modules due to cell temperatures, and the Joule effect in the DC and AC cables. Four SG2500-HV-20 inverters will be needed to connect 29 modules per string and 555 strings in parallel, as shown in the single-line diagram (Figure 17).

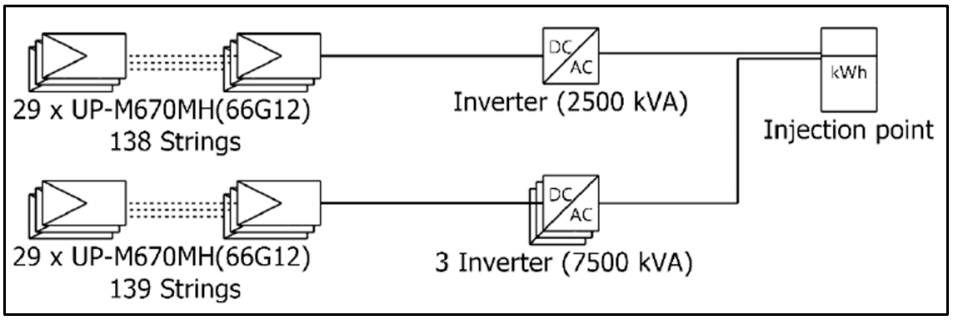

Figure 17. Single-line PV system (extracted from PVsyst v8).

In anticipation of the existence of shading, the PV site was modeled by inserting a structure corresponding to the MSW gasification plant into the 3D analysis system, as it is expected that they will operate in the same place (Figure 6). Although the gasification plant is positioned in the opposite direction to the North-facing faces of the PV modules, shading still occurs. This is reflected in the system's new solar path (Figure 18). Therefore, although reduced, shading occurs from 4:30 p.m. onwards in January, February, March, October, November, and December.

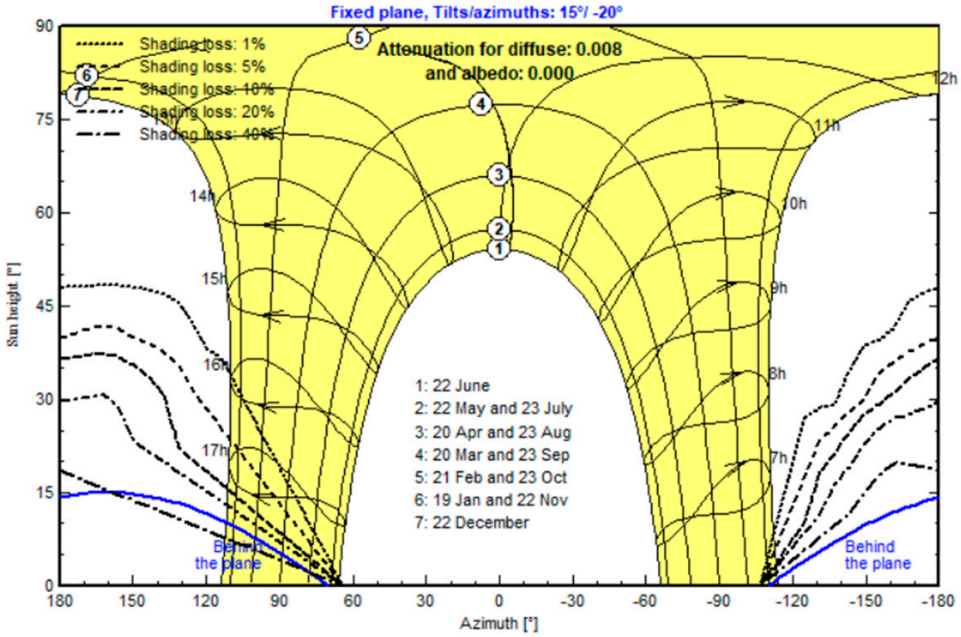

Figure 18. Solar path of the PV system with the presence of an MSW gasification plant (Shading losses from 1% to 40%).

3.2.2. GHG Savings in the PV System

In addition to the MSW gasification-related GHG savings, the GHG emissions savings were estimated using Equation (4), which compares the life-cycle emissions (LCE) of grid-supplied electricity with that of PV-generated electricity. LCE represents the CO_2 emissions associated with a given energy source over its entire life cycle—including installation, production, operation, maintenance, and disposal.

$$PV\ CO_2\ balance = E_{grid} \times Project\_life \times \left(LCE_{grid} - LCE_{PV}\right) \quad (4)$$

where

$PV\ CO_2\ balance$—Total amount of CO_2 emissions avoided by replacing grid-supplied electricity with PV-generated electricity (t CO_2).
E_{grid}—Annual electricity generation from the PV system that would otherwise be drawn from the grid (MWh).
$Project\_life$—Expected operational lifetime of the PV system (yr).
LCE_{grid}—Life-cycle CO_2 emissions intensity of grid electricity (includes extraction, generation, transmission, etc.) (t CO_2/MWh), based on data from sources such as Carbon Trust and ecoinvent v3.9.
LCE_{PV}—Life-cycle CO_2 emissions intensity of the PV-generated electricity (includes panel manufacture, transport, installation, O&M, and end-of-life) (t CO_2/MWh), using global averages provided by the IPCC and available via PVsyst v8.

For an annual E_{grid} of 20,653 MWh, a project lifetime of 25 years, a grid LCE of 412 g CO_2/kWh, and a corresponding LCE_{PV}, the calculation yields an approximate reduction of 395 t CO_2 per year.

This savings estimate reflects the benefits of substituting electricity from the current regional energy mix with that produced by our hybrid system (comprising both PV and MSW gasification). Notably, conventional power generation technologies—such as diesel generators—often exhibit emission intensities between 800 and 1200 g CO_2/kWh. Therefore, the hybrid system not only achieves a measurable annual reduction in CO_2 emissions but also offers a competitive environmental advantage compared to fossil-fuel-based

technologies. Recent studies in similar developing regions have reported relative CO_2 reductions of approximately 20–25% when adopting hybrid renewable systems [16].

3.3. Hybrid System

HOMER Pro v3.16.2 software was employed to simulate the hybrid system, comprising the MSW gasifier, photovoltaic array, and water electrolysis unit for H_2 production. The simulation evaluated system and grid performance in meeting the electricity demand of the Lobito coastal region in Angola, where the peak load is estimated at approximately 700 MW.

3.3.1. MSW Gasification

In terms of the MSW gasification generator configured in HOMER Pro v3.16.2, the results were 4.8 MW of power and 42 GWh/year of electricity for continuous operation throughout the year.

3.3.2. PV System

The PV system was configured considering the data obtained from PVsyst v8. The HOMER Pro v3.16.2 results were a nominal power of 10.784 MW, operating at 4402 h/year, with an LCOE of 0.11 USD/kWh (Figure 19).

(**A**)

Quantity	Value	Units
Rated Capacity	10,784	kW
Mean Output	2,318	kW
Mean Output	55,623	kWh/d
Capacity Factor	21.5	%
Total Production	20,302,259	kWh/yr

Quantity	Value	Units
Minimum Output	0	kW
Maximum Output	13,174	kW
PV Penetration	0	%
Hours of Operation	4,402	hrs/yr
Levelized Cost	0.108	$/kWh
Clipped production	0	kWh

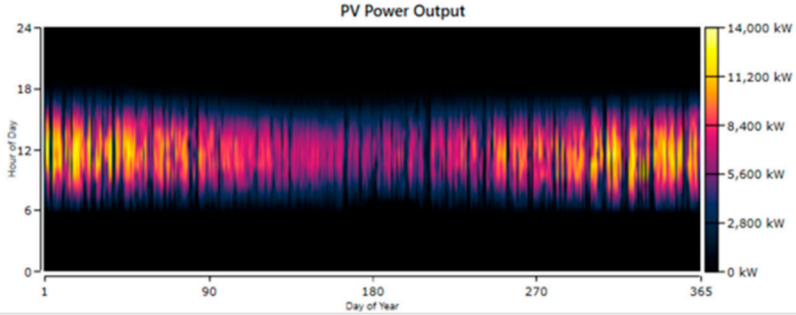

(**B**)

Quantity	Inverter	Rectifier	Units
Capacity	10,823	10,823	kW
Mean Output	2,197	0	kW
Minimum Output	0	0	kW
Maximum Output	10,823	0	kW
Capacity Factor	20.3	0	%

Quantity	Inverter	Rectifier	Units
Hours of Operation	4,402	0	hrs/yr
Energy Out	19,245,873	0	kWh/yr
Energy In	20,258,813	0	kWh/yr
Losses	1,012,941	0	kWh/yr

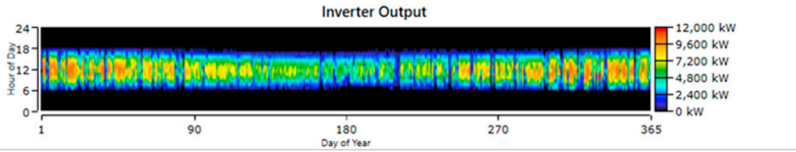

Figure 19. (**A**) PV system electrical production and (**B**) inverter output, as simulated in HOMER Pro v3.16.2.

Figure 19 clearly shows the presence of non-linear solar radiation throughout the day, between 6 a.m. and 6 p.m., hence the black spots throughout the day, which are the result of the system being shaded, among other factors.

As with the PV modules, the results of the system's inverter are shown in Figure 19.

3.3.3. Electrolyzer and Fuel Cell

Regarding the electrolysis of water to generate green H_2, it should be noted that of the 5 MW configured, the renewable electricity generation system only provided an average input of 5.53 kW to the electrolysis, with a maximum power of 1.8 MW. This resulted in a short operational period for this system (Figure 20).

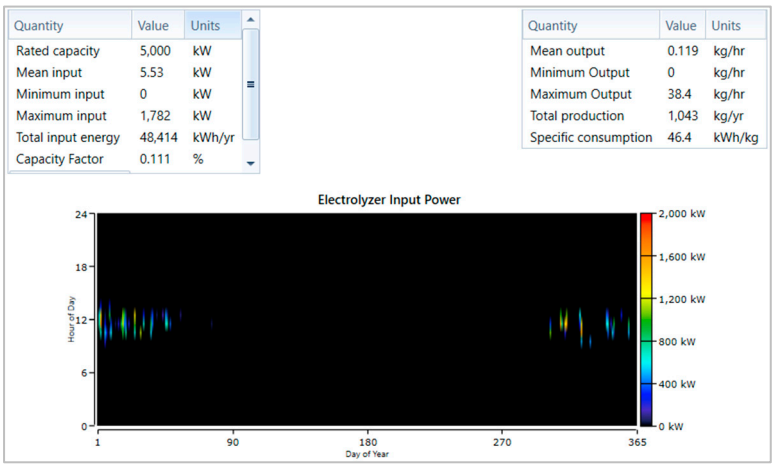

Figure 20. Results of water electrolysis for H_2 generation.

Figures 21 and 22 show that H_2 production occurred over a very short period at the beginning and end of the year, when the system generated some excess electricity. This excess was fed to the electrolyzer, resulting in a total generation of 48 MWh/year of electricity.

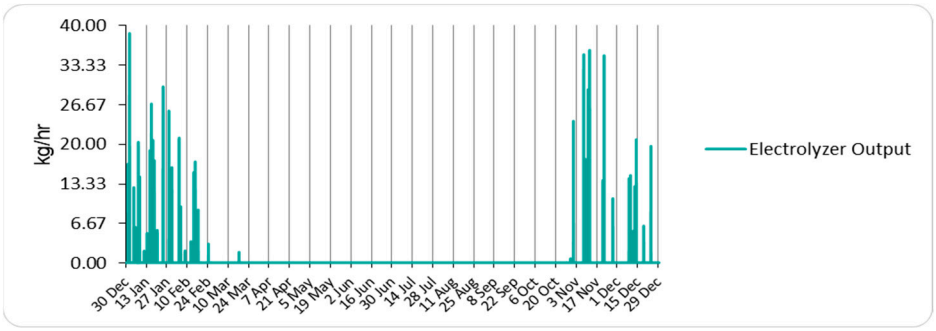

Figure 21. Data obtained on H_2 production by the electrolyzer.

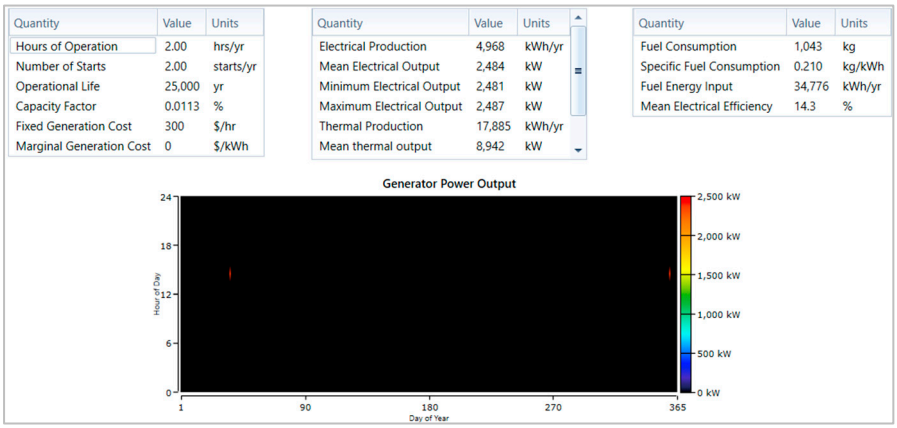

Figure 22. Data obtained from fuel cell operation.

These data suggest that it would not be feasible to install a water electrolysis system to generate green H_2 in the current circumstances of the study region. There is no generation of excess electricity, since almost all the energy produced, both by the gasification of MSW and by the PV system, is injected into the grid.

This limitation highlights the need for future investments in renewable energy infrastructure to achieve surplus electricity, enabling the viability of advanced applications such as hydrogen generation. For now, the focus should be on addressing immediate energy needs and reducing dependence on non-renewable energy sources.

3.3.4. Hybrid System Behavior and Its Impact on the Power Grid

From the above, the PV system generates 20 GWh/year, the MSW gasification generates 42 GWh/year, and the fuel cell generates 5 MWh/year of electric energy. Since the load has a peak energy demand of 10.6 GWh/day, this hybrid system does not prove sufficient to meet a relatively high fraction of the load's power, although it is an output that supplies a considerable number of households.

Considering an average per capita power requirement of 1.5 kW for the study region and assuming that each household comprises, on average, four persons, the total annual electricity production is calculated to supply approximately 1186 households. We acknowledge that household power consumption can vary depending on the number of residents and specific usage patterns. Thus, under alternative assumptions - for instance, if a household consisted of fewer or more than four persons - this number might change accordingly. This estimation serves as a baseline scenario that can be adjusted to suit local demographics and consumption profiles.

Figure 23 shows the summary of electricity generation and its distribution to the loads (households and electrolyzer).

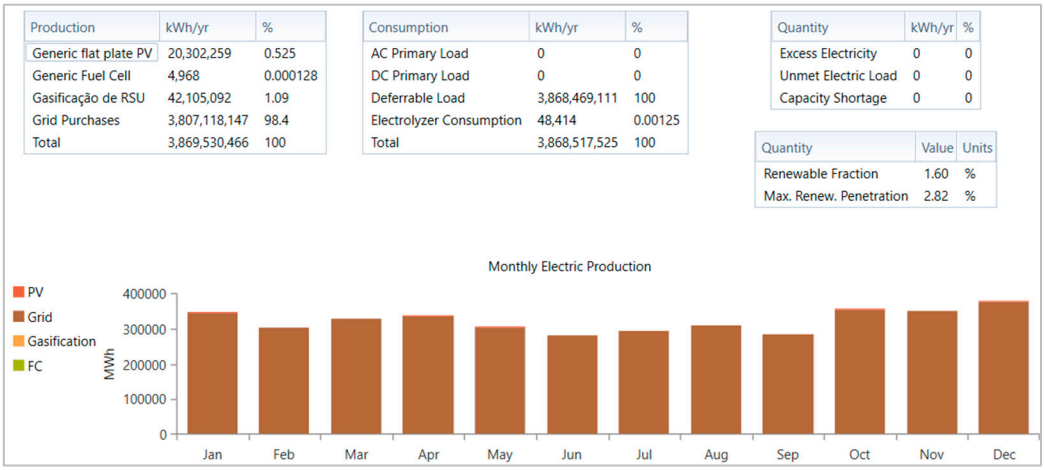

Figure 23. Results on the generation and distribution of electricity from the hybrid system.

As can be seen in Figure 23, there is no excess electricity, since all the energy is injected into the grid, with a maximum penetration of 2.82% throughout the year, and the rest of the electricity is bought to meet the remaining unmet loads, which means that there is no sale of electricity to the grid. Based on the results, the system could be scaled up to larger production capacities, thereby having a more significant impact on the electrical grid. Additionally, the system could be expanded by increasing the collection of MSW from neighboring cities such as Catumbela, Benguela, and Baía Farta. This would not only ensure a greater supply of electricity but also contribute to a more sustainable environment in these areas, as MSW management remains a widespread challenge in Angola.

The current context of the studied region has a negative deficit in electricity supply, which makes it necessary, initially, to try to electrify the entire region, and only after that will it be possible to have excess production if more investment is made in the electricity production infrastructure. Only then will it make sense to invest in the different vectors of electricity, i.e., systems for storing excess electricity, for example, by injecting it into a water electrolysis system to generate green H_2.

3.3.5. Some Economic and Environmental Aspects of the Hybrid System

In the investment assessment, like the operational simulations in HOMER Pro v3.16.2 using data results from Aspen Plus v11.0 and PVsyst v8, additional information was entered regarding the fuel cell, electrolyzer, and H_2 tank. This data was sourced from HOMER Pro v3.16.2 and the US Department of Energy's report on the cost of fuel cells, electrolyzers, and H_2 storage tanks [39]. Table 8 summarizes the investment analysis of the hybrid system under the operating conditions considered in this section.

Table 8. Hybrid system investment analysis summary.

Metric	Value
Investment capital (USD)	67 million
O&M costs (USD)	497 million
Price of selling electricity to the grid (USD/kWh)	0.18
Discount rate (%)	10
LCOE (USD/kWh)	0.1792
Simple payback (years)	~9
Updated payback (years)	~16
Analysis time (years)	25

Assuming a subsidized electricity price of 0.18 USD/kWh and a 10% discount rate over a 25-year analysis period, the discounted payback period is approximately 16 years. This extended payback period is primarily due to the inclusion of the green H_2 production and conversion system, which is not economically viable due to its low H_2 production rate. As a result, it imposes a financial burden on the hybrid system. However, excluding the H_2 production system and maintaining only MSW gasification and PV plants would shorten the payback period to 11 years.

Nevertheless, the system provides significant positive externalities by creating jobs and contributing to increasing the energy mix and electrification and reducing household energy poverty.

3.4. Comparison with Similar Hybrid Systems in Developing Regions

To assess the feasibility of the proposed hybrid system, its performance was compared with similar studies conducted in developing regions. These comparisons provide insights into the technical, economic, and environmental dimensions of integrating MSW gasification with PV systems.

3.4.1. Technical Performance

Campos et al. [15] analyzed a PV–biomass system in Brazil, achieving an energy efficiency of 17.43%. Similarly, Yew et al. [17] in Malaysia modeled a hybrid solar–biomass system with a total installed capacity of 4.075 kW (PV) and 2.100 kW (biomass gasifier), and Ribó-Pérez et al. [16] evaluated a biomass gasification-based hybrid microgrid in Zambia, demonstrating its effectiveness in providing decentralized electricity to rural communities. Their system achieved high operational reliability with a comparable energy yield to other PV–biomass hybrid models. In comparison, the system proposed in this study generates

62 GWh/year, demonstrating its feasibility for large-scale implementation. However, the challenges associated with MSW composition and variability may require further process optimization.

3.4.2. Economic Viability

The LCOE obtained in this study is 0.1792 USD/kWh, which is higher than the 0.034 USD/kWh reported by Campos et al. [15] in Brazil, the 0.10 USD/kWh estimated for Malaysia by Yew et al. [17], and the Zambian system's LCOE analyzed by Ribó-Pérez et al. [16], which remained below 0.12 USD/kWh, benefiting from simplified biomass processing. This difference is primarily due to the additional costs of MSW processing and hydrogen production. However, when excluding the hydrogen production system, the payback period is reduced from 16 to 11 years, aligning with the values reported in Egypt [12] and Zambia [16] of 12 years and 10 years, respectively.

3.4.3. Environmental Impact

The proposed system in this study reduces CO_2 emissions by 42,000 t/year from MSW gasification and 395 t/year from PV production—comparable to the reductions observed in similar hybrid PV–biomass projects. Ribó-Pérez et al. [16] also highlighted the role of hybrid biomass-based systems in achieving emissions reductions of 20–25% compared to conventional fossil-fuel generation.

4. Conclusions

This study assessed the potential of a hybrid renewable energy system integrating MSW gasification and a PV system to address energy challenges in Lobito, Angola. The gasification process converts MSW into syngas through thermal decomposition under controlled conditions. The PV system supplements this process by harnessing solar energy, optimized through precise system design and simulation to maximize energy output under local solar conditions.

The integration of the MSW gasification plant and solar PV park addressed critical energy challenges by ensuring continuous power generation and reducing reliance on fossil fuels. The system generated 62 GWh/year, with a penetration rate of 2.80%, supplying electricity to 1186 households while achieving an LCOE of 0.1792 USD/kWh and a payback period of 16 years.

From an environmental perspective, the system reduced CO_2 emissions by 42,000 t/year from MSW gasification and 395 t/year from PV production, demonstrating its potential for decreasing GHG emissions and mitigating climate change related to waste-related pollution. The deployment of MSW gasification also highlighted the role of waste-to-energy technologies in enhancing urban waste management and promoting a circular economy.

However, the lack of surplus electricity for green hydrogen production indicates the need for further infrastructure investments to increase energy production if H_2 is intended to be produced. This limitation highlights a key area for future research: scaling up hybrid systems to achieve excess energy for advanced applications such as hydrogen generation and storage. Additionally, studies on optimizing syngas cleaning processes could enhance the efficiency and longevity of gasification systems.

While this study focused on the technical and economic feasibility of the proposed hybrid system, future research should explore maintenance and operational challenges, particularly for MSW gasification. These factors are critical for ensuring long-term economic viability and practical implementation.

Furthermore, the payback period of 16 years is primarily due to the inclusion of the hydrogen production system, which is not currently economically viable. When excluding

the hydrogen production component, the payback period is reduced to 11 years, making the system significantly more attractive for investment and implementation in similar regions.

It is also recommended that future work include additional local surveys and waste characterization studies to further refine the proximate analysis and the LHV of MSW.

In conclusion, this research provides a scalable framework for integrating renewable energy sources in developing regions, offering a pathway to reduce energy poverty, improve environmental quality, and achieve sustainable development goals, such as good health and well-being, affordable and clean energy, decent work and economic growth, and industry, innovation, and infrastructure. The findings are intended to inform policymakers, investors, and researchers in the development of hybrid energy solutions tailored to local contexts.

Author Contributions: Conceptualization, S.J., N.A. and N.L.; Methodology, S.J., N.A. and N.L.; Software, S.J.; Supervision, N.A. and N.L.; Writing—Original Draft, S.J.; Writing—Review and Editing, N.A. and N.L. All authors have read and agreed to the published version of the manuscript.

Funding: This research received no external funding.

Institutional Review Board Statement: Not applicable.

Informed Consent Statement: Not applicable.

Data Availability Statement: The original contributions presented in this study are included in the article. Further inquiries can be directed to the corresponding author.

Acknowledgments: Salomão Muquepe Joaquim acknowledges the Government of Angola, Ministério do Ensino Superior, Ciência, Tecnologia e Inovação, for the MSc. fellowship attributed in the framework of the Presidential Decree number 67/19 of 22 February.

Conflicts of Interest: The authors declare that they have no known competing financial interests or personal relationships that could have appeared to influence the work reported in this paper.

Abbreviations

The following abbreviations are used in this manuscript:

AC	Alternating Current
CCE	Carbon Conversion Efficiency
CGE	Cold Gas Efficiency
DC	Direct current
DW	Dry weight
ER	Equivalence Ratio
IPCC	Intergovernmental Panel on Climate Change
LCE	Life-Cycle Emissions
LCOE	Levelized Cost of Energy
LHV	Low Heating Value
MPPT	Maximum Power Point Tracking
MSW	Municipal Solid Waste
DW	Dry weight
PR	Performance Ratio
PV	Photovoltaic
STC	Standard Test Conditions
Syngas	Synthesis Gas
UN	United Nations
Wt%	Weight percent
PR	Performance Ratio

References

1. Our World in Data. Global Primary Energy Consumption by Source. 2023. Available online: https://ourworldindata.org/grapher/global-energy-consumption-source?tab=table&time=latest (accessed on 18 November 2024).
2. Ritchie, H.; Roser, M. Energy | Angola: Energy Country Profile. Our World in Data. Available online: https://ourworldindata.org/energy (accessed on 18 November 2024).
3. Fonseca, M. Angola—Energy. Angola—Country Commercial Guide. Available online: https://www.trade.gov/country-commercial-guides/angola-energy (accessed on 3 March 2023).
4. Centers for Disease Control and Prevention. CDC in Angola | CDC. Available online: https://www.cdc.gov/global-health/countries/angola.html?CDC_AAref_Val=https://www.cdc.gov/globalhealth/countries/angola/default.htm (accessed on 25 January 2023).
5. Mukherjee, C.; Denney, J.; Mbonimpa, E.G.; Slagley, J.; Bhowmik, R. A review on municipal solid waste-to-energy trends in the USA. *Renew. Sustain. Energy Rev.* **2020**, *119*, 109512. [CrossRef]
6. Bin Nadeem, T.; Siddiqui, M.; Khalid, M.; Asif, M. Distributed energy systems: A review of classification, technologies, applications, and policies. *Energy Strateg. Rev.* **2023**, *48*, 101096. [CrossRef]
7. Ali, F.; Dawood, A.; Hussain, A.; Alnasir, M.H.; Khan, M.A.; Butt, T.M.; Janjua, N.K.; Hamid, A. Fueling the future: Biomass applications for green and sustainable energy. *Discov. Sustain.* **2024**, *5*, 156. [CrossRef]
8. Freris, L.; Infield, D. *Renewable Energy in Power Systems*, 1st ed.; John Wiley & Sons: Chichester, UK, 2008.
9. Soudagar, M.E.M.; Ramesh, S.; Khan, T.Y.; Almakayeel, N.; Ramesh, R.; Ghazali, N.N.N.; Cuce, E.; Shelare, S. An overview of the existing and future state of the art advancement of hybrid energy systems based on PV-solar and wind. *Int. J. Low-Carbon Technol.* **2024**, *19*, 207–216. [CrossRef]
10. Lee, J.; Lin, K.Y.A.; Jung, S.; Kwon, E.E. Hybrid renewable energy systems involving thermochemical conversion process for waste-to-energy strategy. *Chem. Eng. J.* **2023**, *452*, 139218. [CrossRef]
11. Alhijazi, A.A.K.; Almasri, R.A.; Alloush, A.F. A Hybrid Renewable Energy (Solar/Wind/Biomass) and Multi-Use System Principles, Types, and Applications: A Review. *Sustainability* **2023**, *15*, 16803. [CrossRef]
12. El-Sattar, H.A.; Kamel, S.; Sultan, H.M.; Zawbaa, H.M.; Jurado, F. Optimal design of Photovoltaic, Biomass, Fuel Cell, Hydrogen Tank units and Electrolyzer hybrid system for a remote area in Egypt. *Energy Rep.* **2022**, *8*, 9506–9527. [CrossRef]
13. El-Sattar, H.A.; Kamel, S.; Hassan, M.H.; Jurado, F. Optimal sizing of an off-grid hybrid photovoltaic/biomass gasifier/battery system using a quantum model of Runge Kutta algorithm. *Energy Convers. Manag.* **2022**, *258*, 115539. [CrossRef]
14. Cano, A.; Arévalo, P.; Jurado, F. Energy analysis and techno-economic assessment of a hybrid PV/HKT/BAT system using biomass gasifier: Cuenca-Ecuador case study. *Energy* **2020**, *202*, 117727. [CrossRef]
15. Campos, C.F.C.; de Sá Machado, V.A.; Soares, L.O.; Boloy, R.A.M. Techno-economic analysis and eco-efficiency indicators of a biomass-solar hybrid renewable energy system for João Pinheiro City. *Discov. Sustain.* **2024**, *5*, 41. [CrossRef]
16. Ribó-Pérez, D.; Herraiz-Cañete, Á.; Alfonso-Solar, D.; Vargas-Salgado, C.; Gómez-Navarro, T. Modelling biomass gasifiers in hybrid renewable energy microgrids; a complete procedure for enabling gasifiers simulation in HOMER. *Renew. Energy* **2021**, *174*, 501–512. [CrossRef]
17. Yew, P.J.; Chaulagain, D.; Same, N.N.; Park, J.; Lim, J.-O.; Huh, J.-S. Optimal Hybrid Renewable Energy System to Accelerate a Sustainable Energy Transition in Johor, Malaysia. *Sustainability* **2024**, *16*, 7856. [CrossRef]
18. Macías, R.J.; Ceballos, C.; Ordonez-Loza, J.; Ortiz, M.; Gómez, C.A.; Chejne, F.; Vélez, F. Evaluation of the performance of a solar photovoltaic—Biomass gasifier system as electricity supplier. *Energy* **2022**, *260*, 125046. [CrossRef]
19. Xin, Y.; Zhang, W.; Chen, F.; Xing, X.; Han, D.; Hong, H. Integrating solar-driven biomass gasification and PV-electrolysis for sustainable fuel production: Thermodynamic performance, economic assessment, and CO_2 emission analysis. *Chem. Eng. J.* **2024**, *497*, 153941. [CrossRef]
20. Pan, Z.; Chan, W.P.; Veksha, A.; Giannis, A.; Dou, X.; Wang, H.; Lisak, G.; Lim, T.T. Thermodynamic analyses of synthetic natural gas production via municipal solid waste gasification, high-temperature water electrolysis and methanation. *Energy Convers. Manag.* **2019**, *202*, 112160. [CrossRef]
21. Balan, D.-C.; Balan, S.-M.; Szakacs, J. Technical-Economic Analysis of a Hybrid Energy Systems Composed of PV and Biomass Obtained from Municipal Solid Waste Connected to the Grid. *Proceedings* **2020**, *63*, 9. [CrossRef]
22. Sun, Y.; Tang, Y. Municipal solid waste gasification integrated with water electrolysis technology for fuel production: A comparative analysis. *Chem. Eng. Res. Des.* **2023**, *191*, 14–26. [CrossRef]
23. Huld, T.; Müller, R.; Gambardella, A. A new solar radiation database for estimating PV performance in Europe and Africa. *Solar Energy* **2012**, *86*, 1803–1815. [CrossRef]
24. Seo, Y.-C.; Alam, M.T.; Yang, W.-S. Gasification of Municipal Solid Waste. In *Gasification for Low-Grade Feedstock*; InTech: London, UK, 2018. [CrossRef]

25. Timsina, R.; Thapa, R.K.; Eikeland, M.S. Aspen Plus simulation of biomass gasification for different types of biomass. In Proceedings of the 60th SIMS Conference on Simulation and Modelling SIMS, Västerås, Sweden, 12–16 August 2020; Linköping Electronic Conference Proceedings; Volume 170, pp. 151–157. [CrossRef]
26. Işık, K.E.; Dogru, M.; Erdem, A. Gasification of MDF residue in an updraft fixed bed gasifier to produce heat and power via an ORC turbine. *Waste Manag.* **2023**, *169*, 43–51. [CrossRef]
27. Begum, S.; Rasul, M.G.; Akbar, D. A numerical investigation of municipal solid waste gasification using aspen plus. *Procedia Eng.* **2014**, *90*, 710–717. [CrossRef]
28. Moshi, R.E.; Jande, Y.A.C.; Kivevele, T.T.; Kim, W.S. Simulation and performance analysis of municipal solid waste gasification in a novel hybrid fixed bed gasifier using Aspen plus. *Energy Sources Part A* **2020**, *46*, 13856–13868. [CrossRef]
29. Dong, J. MSWs Gasification with Emphasis on Energy, Environment and Life Cycle Assessment. Ph.D. Thesis, Chemical and Process Engineering, Ecole des Mines d'Albi-Carmaux, Albi, France, Institute for Thermal Power Engineering, Zhejiang University, Hangzhou, China, 2016. Available online: https://tel.archives-ouvertes.fr/tel-01540764 (accessed on 9 June 2025).
30. Hadi, N.S. *Chapter Three (Solid Waste Management): Physical, Chemical, and Biological Properties of Municipal Solid Waste*; University of Babylon-College of Engineering: Babylon, Iraq, 2023. Available online: https://www.uobabylon.edu.iq/eprints/publication_2_9209_659.pdf (accessed on 14 April 2023).
31. Phyllis2—ECN Phyllis Classification. Database for the Physico-Chemical Composition of (Treated) Lignocellulosic Biomass, Micro- and Macroalgae, Various Feedstocks for Biogas Production and Biochar. Available online: https://phyllis.nl/Browse/Standard/ECN-Phyllis (accessed on 14 April 2023).
32. JICA; TEPSCO; IIEP. The Project for Power Development Master Plan in the Republic of Angola. Available online: https://rise.esmap.org/data/files/library/angola/Electricity%20Access/Angola_The%20Project%20for%20Power%20Development%20Master%20Plan%20in%20the%20Republic%20of%20Angola_2018.pdf (accessed on 18 April 2025).
33. Rey, J.R.C.; Longo, A.; Rijo, B.; Pedrero, C.M.; Tarelho, L.A.C.; Brito, P.S.D.; Nobre, C. A review of cleaning technologies for biomass-derived syngas. *Fuel* **2024**, *377*, 132776. [CrossRef]
34. Pudi, A.; Rezaei, M.; Signorini, V.; Andersson, M.P.; Baschetti, M.G.; Mansouri, S.S. Hydrogen sulfide capture and removal technologies: A comprehensive review of recent developments and emerging trends. *Sep. Purif. Technol.* **2022**, *298*, 121448. [CrossRef]
35. Intergovernmental Panel on Climate Change (IPCC). *2006 IPCC Guidelines for National Greenhouse Gas Inventories*; Prepared by the National Greenhouse Gas Inventories Programme; Eggleston, H.S., Buendia, L., Miwa, K., Ngara, T., Tanabe, K., Eds.; Institute for Global Environmental Strategies (IGES): Kanagawa, Japan, 2006; Volume 2. Available online: https://www.ipcc-nggip.iges.or.jp/public/2006gl/vol2.html (accessed on 5 June 2025).
36. International Energy Agency (IEA). *CO_2 Emissions from Fuel Combustion 2019*; IEA: Paris, France, 2019. [CrossRef]
37. Arena, U. Process and technological aspects of municipal solid waste gasification. A review. *Waste Manag.* **2012**, *32*, 625–639. [CrossRef]
38. Bianco, I.; Panepinto, D.; Zanetti, M. Environmental Impacts of Electricity from Incineration and Gasification: How the LCA Approach Can Affect the Results. *Sustainability* **2022**, *14*, 92. [CrossRef]
39. U.S. Department of Energy. Comparison of Fuel Cell Technologies. 2016. Available online: https://www.energy.gov/eere/fuelcells/articles/comparison-fuel-cell-technologies-fact-sheet (accessed on 18 April 2025).